ACTA ASTRONOMICA
Vol. **64** (2014) pp. 1–1

Ultra-Short-Period Binary Systems in the OGLE Fields Toward the Galactic Bulge*

I. Soszyński[1], K. Stępień[1], B. Pilecki[1,2], P. Mróz[1], A. Udalski[1], M.K. Szymański[1], G. Pietrzyński[1,2], Ł. Wyrzykowski[1,3], K. Ulaczyk[1], R. Poleski[1,4], S. Kozłowski[1], P. Pietrukowicz[1], J. Skowron[1] and M. Pawlak[1]

[1] Warsaw University Observatory, Al. Ujazdowskie 4, 00-478 Warszawa, Poland
e-mail: soszynsk@astrouw.edu.pl
[2] Universidad de Concepción, Departamento de Astronomia, Casilla 160–C, Concepción, Chile
[3] Institute of Astronomy, University of Cambridge, Madingley Road, Cambridge CB3 0HA, UK
[4] Department of Astronomy, Ohio State University, 140 W. 18th Ave., Columbus, OH 43210, USA

Received

ABSTRACT

We present a sample of 242 ultra-short-period ($P_{\rm orb} < 0.22$ d) eclipsing and ellipsoidal binary stars identified in the OGLE fields toward the Galactic bulge. Based on the light curve morphology, we divide the sample into candidates for contact binaries and non-contact binaries. In the latter group we distinguish binary systems consisting of a cool main-sequence star and a B-type subdwarf (HW Vir stars) and candidates for cataclysmic variables, including five eclipsing dwarf novae. One of the detected eclipsing binary systems – OGLE-BLG-ECL-000066 – with the orbital period below 0.1 d, likely consists of M dwarfs in a nearly contact configuration. If confirmed, this would be the shortest-period M-dwarf binary system currently known. We discuss possible evolutionary mechanisms that could lead to the orbital period below 0.1 d in an M-dwarf binary.

Key words: *binaries: eclipsing – stars: low-mass – novae, cataclysmic variables – stars: individual: OGLE-BLG-ECL-000066*

1. Introduction

In recent years the list of known eclipsing binary systems with very short periods has been substantially extended. It is known for more than two decades (Rucin-

*Based on observations obtained with the 1.3-m Warsaw telescope at the Las Campanas Observatory of the Carnegie Institution for Science.

ski 1992) that contact binaries have a sharp cut-off at ~ 0.22 d in the period distribution, and very few systems have periods significantly below this limit. For years, the shortest-period known binary system with M-dwarf components was OGLE BW3 V38 ($P = 0.1984$ d) discovered by Udalski *et al.* (1995) and studied in detail by Maceroni and Rucinski (1997). This record was beaten by Norton *et al.* (2007), who reported the discovery of a binary system with main sequence components on a $P = 0.1926$-d orbit. Then, rich samples of ultra-short period binaries were published by Norton *et al.* (2011), Nefs *et al.* (2012), Lohr *et al.* (2013), and recently by Drake *et al.* (2014), who identified as many as 367 binary systems with periods below 0.22 days using photometric databases collected by the Catalina Surveys. Until now, the shortest known period of the M dwarf binary systems was $P = 0.1122$ d (Nefs *et al.* 2012).

Two main hypotheses have recently been proposed to explain the short-period cut-off in contact eclipsing binaries. Stępień (2006b) argued that the short-period limit of contact binaries may be caused by the fact that the initially detached systems with low-mass components do not have time to reach the Roche lobe overflow within the age of the Universe. An existence of a lower limit about 2 d for the initial orbital period is essential for this explanation. It results from a binary star formation mechanism in which a binary is formed due to a fragmentation of a protostellar cloud (Bonnell 1994, Machida *et al.* 2008, Kratter *et al.* 2010). So, a new born cool binary consists of two T Tau stars and its orbit must be wide enough to accommodate components with radii of a few solar radii. A similar low limit for a period of young binaries is expected when the mechanism called Kozai cycles with a tidal friction (KCTF) operates on a binary with an initially longer period (Fabrycky and Tremaine 2007, Perets and Fabrycky 2009, Naoz and Fabrycky 2014). For components with masses close to 0.2 $M_{\odot}$, the low limit for the initial period is somewhat lower – around 1.5 d (Nefs *et al.* 2012). This does not mean, of course, that shorter initial periods are completely forbidden. The KCTF mechanism can produce shorter periods under exceptional circumstances and also a close approach with another body can "harden" a binary, shortening significantly its period (e.g. Hypki and Giersz 2013). Nevertheless, young binaries with very short periods are expected to be rare.

On the other hand, Jiang *et al.* (2012) noted that existence of detached and semi-detached binary systems with periods below the short-period limit are in conflict with the suggestion of Stępień (2006b). The existence of systems with such short periods indicates that some of the binaries may have short periods at their birth or that they may experience a much higher angular momentum loss than assumed by Stępień (2006b). According to Jiang *et al.* (2012), the short-period limit of contact binaries results from a limit for the mass of the primary component. For initial primary mass lower than 0.63 $M_{\odot}$, the mass transfer that starts, when the primary reaches its Roche lobe, is dynamically unstable, which quickly leads to the common envelope binary and the coalescence of both components. Only binaries

with the primary mass higher than 0.63 $M_{\odot}$ may form long-lived W UMa stars and their orbital periods are longer than about 0.22 d. This explanation may be invoked if, indeed, a substantial fraction of young binaries has very short periods of 1 d or less.

The mystery of the short-period cut-off could be solved by detailed examination of the ultra-short-period binaries. The relative numbers of contact versus detached binaries and their period distribution may be an important constraint on models of the formation and migration history in low-mass binary systems. Analysis of the orbital period changes could answer the question of whether the angular momentum loss in low-mass close binaries is so fast that such systems quickly merge and form single stars (Jiang *et al.* 2012) or, on the contrary, the momentum loss is so feeble that any M-dwarf binary had no time to form contact system (Stępień 2006b). For binaries with orbits tidally tightened by the KCTF mechanism the third, circumbinary, objects should also be detected through the timing analysis.

Therefore, it is essential to find as many as possible ultra-short-period M-dwarf binaries to test the predictions of angular momentum loss theories. In the present study we publish the list of 242 binary systems with orbital periods below 0.22 d detected toward the Optical Gravitational Lensing Experiment (OGLE) fields in the Galactic bulge. Our sample consists not only of the M-dwarf binaries, but also of the main-sequence – hot sub-dwarf systems and of cataclysmic variables. One of our objects – OGLE-BLG-ECL-000066 – is probably the shortest-period binary system consisting of two M-dwarfs.

2. Observations and Data Reduction

OGLE is a long-term photometric survey for sky variability operating on the 1.3-m Warsaw Telescope at Las Campanas Observatory, Chile. The observatory is operated by the Carnegie Institution for Science. In this investigation, we used photometric data collected during the third and the fourth phases of the OGLE survey (OGLE-III and OGLE-IV) in the years 2001–2013. Currently, the telescope is equipped with a 32-chip 256 megapixel mosaic camera with 1.4 square degrees field of view. The OGLE survey uses two photometric filters: about 90% of the observations are obtained in the Cousins *I* band, the remaining images were made with the Johnson *V* band. The number of observations substantially varies from field to field: from about 100 to more than 8000 points per light curve.

The short-period eclipsing binary candidates were detected in the area of 182 square degrees covering central regions of the Milky Way. The *I*-band magnitudes in the OGLE-IV database range from about 13 mag to 20.5 mag. Data reduction of the OGLE images is performed using the Difference Image Analysis pipeline (Alard and Lupton 1998, Woźniak 2000). Detailed descriptions of the instrumentation, photometric reductions and astrometric calibrations of the OGLE data are available in Udalski (2003a) and Udalski *et al.* (2008).

3. Selection and Classification of Ultra-Short-Period Binary Systems

The period analysis for nearly 400 million *I*-band light curves collected by OGLE in the Galactic bulge was done using FNPEAKS code[†] written by Z. Kołaczkowski. We searched a frequency space from 0 to 24 d^{-1} with a spacing of 0.00005 d^{-1}. The light curves with the periods below 0.22 d and with the highest signal-to-noise ratio were subjected to visual inspection. Identified variable stars were divided into three groups: eclipsing/ellipsoidal binaries, pulsating stars (in most cases δ Sct stars) and other variables. The latter group contains mostly variables of undetermined types. Some of them may be binary systems or pulsating stars, but we are not able to confidently classify them based solely on the OGLE light curves.

In this paper, we present 242 objects gathered in the first group – containing rather certain cases of short-period eclipsing or ellipsoidal variables. In order to classify our binary systems into different types, each *I*-band light curve was analyzed with the aid of the Wilson-Devinney light curve modeling technique (Wilson and Devinney 1971, hereafter WD code). We have used the procedure developed by Pilecki (2010), see also Pilecki and Stępień (2012). Our method is based on a mixture of standard Monte Carlo approach and the Markov Chain Monte Carlo (MCMC) method. In this approach, model light curves were created using the WD code for a given random parameter set. Then they were compared with the observational data and the reduced χ^2 values were calculated to measure the goodness of the model. The final model was the one with the lowest χ^2 value.

For the purpose of this work the method was simplified, as we did not have radial velocities measured for the stars. In the analysis we included the following parameters: the modified surface potentials Ω_1 and Ω_2, the orbital inclination i, the temperature ratio T_2/T_1 (temperature of the hotter component was fixed), and the phase shift. The period and the reference time of the primary minimum was taken from the Fourier analysis of the light curves, but the phase shift took care of any error in the latter. Also, for each star two mass ratios were tested, one representing the components of equal masses ($q = 1.0$) and the other representing components of unequal masses ($q \sim 0.35$), but they were fixed during the analysis. For individual stars other values of mass ratios were also tested, if needed.

To facilitate the automated search for the best model we divided the sample into two groups – one with narrow eclipses (meaning higher component separation) and no distinct proximity effects visible – detached system candidates, and the other with wider eclipses and a continuous brightness change (with proximity effects) – compact system candidates. For both groups we used a different set of initial parameters and parameter ranges in order to minimize necessary calculations to find the global minimum. For the detached system group, we started from a higher component separation and higher inclination angles and for the compact

[†]see http://helas.astro.uni.wroc.pl/deliverables.php?lang=en&active=fnpeaks

system group from a lower component separation and in a wider range of inclination angles. Also, for some detached systems with extreme ratios of eclipse depths, we changed the initial temperature ratio of the model, and for stars with distinct reflection effect (see Section 5.3) the temperature of the hotter component was set to 30,000 K. In other cases the temperature was set to 5000 K (compact systems) and 6000 K (detached systems), as it has only an indirect influence by the limb darkening coefficients and does not affect much the solution.

The following steps were practically the same for all the stars. Using a slightly modified standard Monte Carlo approach we were looking for the best models in a wide range of parameter space. To avoid situation in which the global minimum is outside the parameter range instead of using the uniform distribution, we were taking values from the normal distribution minimizing this risk. Once about a thousand models are calculated, the range and the central point of the distribution are automatically changed to better cover the parameter ranges for which best models are obtained. Narrowing the parameter ranges (changing the sigma and the central value of the normal distribution) we were able to find a global minimum in the χ^2 plane. Between some steps the MCMC method was also applied to minimize the risk of being stuck at some local minimum. In this method there is no fixed range of parameters and no central point of distribution is used, so after a sufficient steps it may virtually cover the whole range of parameters value. There is a restriction though that makes this method avoid parameter sets that give highly improbable models.

Using this procedure, calculating a few thousand models was in general sufficient to find a global minimum with the enough accuracy and even estimate the errors of the parameters quite reliably (taking into account all the simplifications). For each system the reduced χ^2 values for different mass ratios were compared and the model with lower value was selected as the best one. Calculating models for more values of mass ratios could be done, but the two tested values were sufficient to fulfill the main goal of this analysis – to obtain the approximate parameters and to tell if the stars are in contact or not. Also one must have in mind that the photometric mass ratios are just a rough approximation anyway and that they can be trusted only in some specific cases (contact binaries with total eclipses), since in general one needs a spectroscopic mass ratio. The configuration of the system was determined using the Roche lobe filling factor of the components. Here we measure this factor as a ratio between the polar radius of the star and the polar radius of the corresponding Roche lobe. If these ratios for both components are higher or equal to one, the system is considered as a contact one. These objects display light curves that are characteristic of W UMa-type stars: with similar depths of minima and with continuously changing brightness because of large tidal distortion of the two components. Other cases – semi-detached and detached systems – were grouped into one class – non-contact binaries. Among these objects we could distinguish interesting sub-groups: cataclysmic variables and systems containing

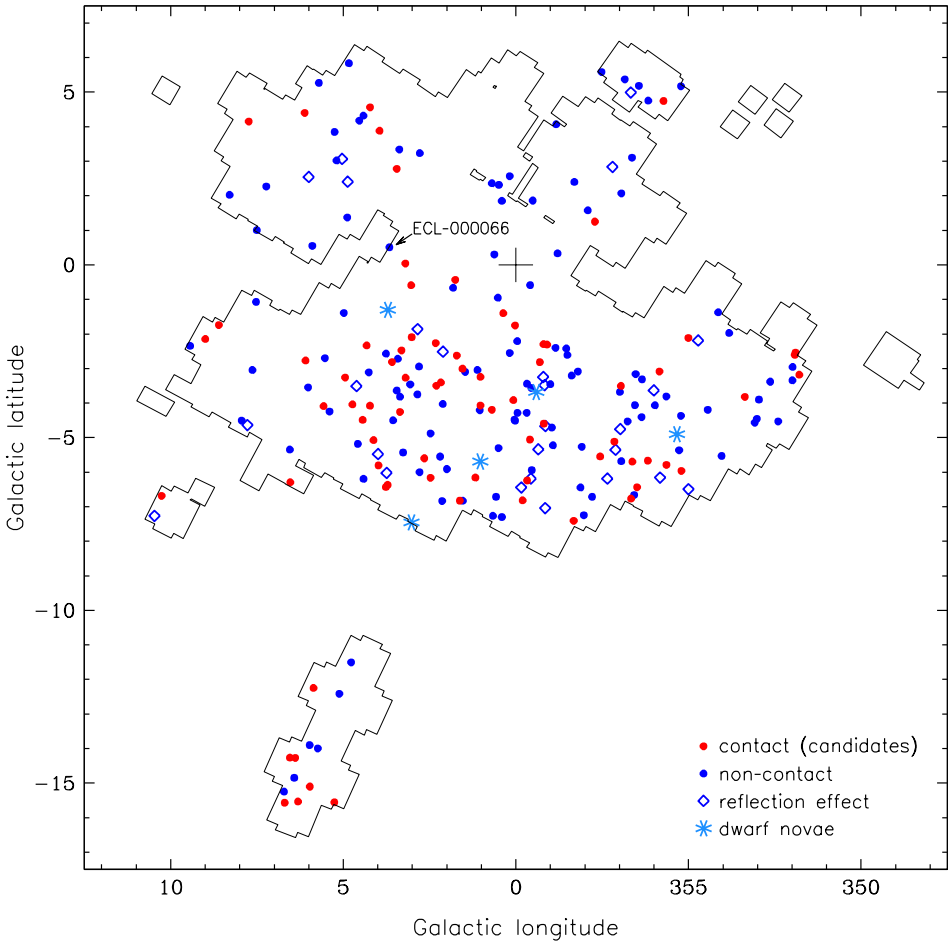

Fig. 1. Spatial distribution of ultra-short-period binary systems in the OGLE fields toward the Galactic bulge. Red points indicate candidates for contact binaries, blue points show positions of non-contact (detached and semi-detached) systems. Stars with strong reflection effect are marked with empty diamonds, dwarf novae are showed with blue stars. Black line show contours of the OGLE fields toward the Galactic bulge.

cool main sequence stars and hot evolved companions. Also, using the inclination parameters and the relative radii of the stars calculated from the potentials, we were able to tell if there are no eclipses at all, and that the brightness change is only or mostly due to the ellipsoidal variation.

4. OGLE Sample of Ultra-Short-Period Binary Systems

The final sample consists of 242 short-period eclipsing and ellipsoidal binary systems detected toward the Galactic bulge. 75 of these objects are candidates for eclipsing contact binaries (W UMa stars), 167 stars are probable semi-detached and detached systems. From the latter group, five stars are dwarf novae, four stars

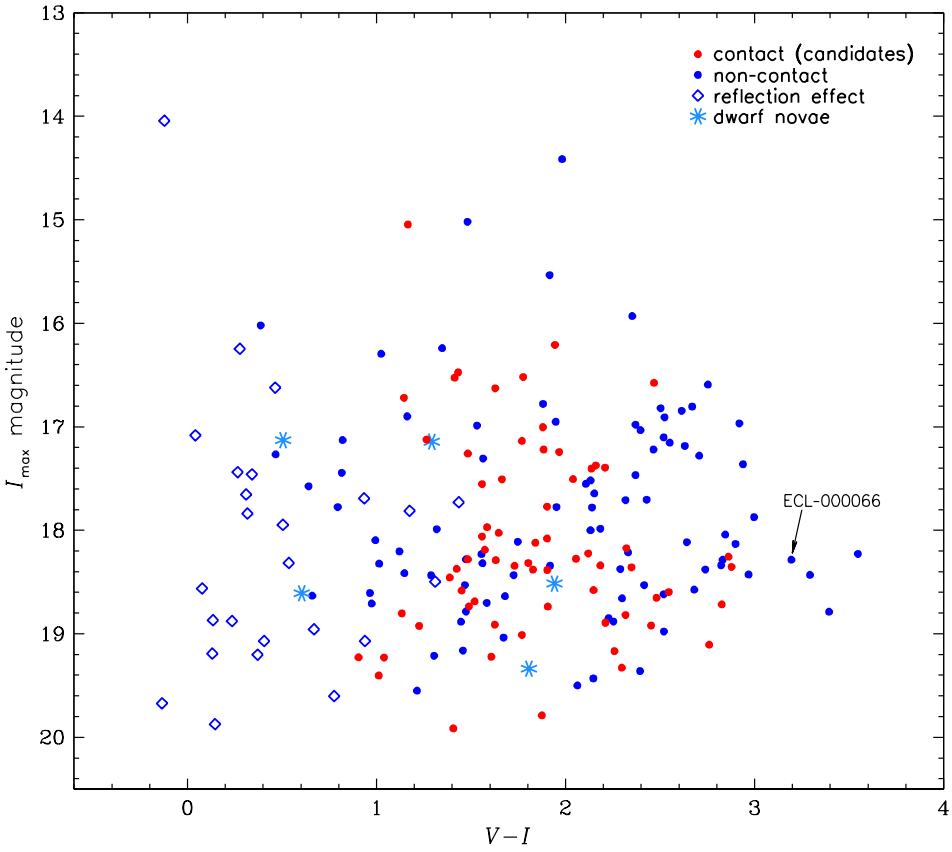

Fig. 2. Color–magnitude diagram for ultra-short-period binary systems. Different symbols have the same meaning as in Fig. 1.

are known Novae and ten other objects are candidates for cataclysmic variables. We provide basic observational parameters of our sample, the OGLE time-series photometry in the *I* and *V* bands and finding charts. These data can be downloaded from the FTP anonymous site:

ftp://ftp.astrouw.edu.pl/ogle/ogle4/OCVS/blg/short_period_ecl/

Eclipsing and ellipsoidal systems were given designations OGLE-BLG-ECL-NNNNNN and OGLE-BLG-ELL-NNNNNN, respectively, where NNNNNN is a six-digit number. This designation scheme will be continued in the OGLE collection of eclipsing and ellipsoidal variables, which will be published in the future. Table 1 contains first 30 lines the file list.dat from the FTP site. For each star we provide its identifiers, J2000 equatorial coordinates, type of variability (C – contact binary, NC – non-contact binary, ELL – ellipsoidal variable, CV – cataclysmic variable), *I*- and *V*-band magnitudes at maximum light, orbital period, primary and secondary eclipse depths in the *I*-band, and epoch of the primary eclipse minimum. The orbital periods were refined with the TATRY code (Schwarzenberg-Czerny 1996).

Table 1

First 30 lines of the file list.dat.

Identifier	OGLE Identifier	R.A. [J2000.0]	Dec [J2000.0]	Type	I_{max} [mag]	V_{max} [mag]	P_{orb} [d]	$A_1(I)$ [mag]	$A_2(I)$ [mag]	T_{min} HJD-2450000
OGLE-BLG-ECL-000001	BLG617.07.79075	17:13:40.94	−30:04:17.2	NC	18.714	–	0.20903930	0.916	0.538	5000.15657
OGLE-BLG-ECL-000002	BLG617.11.65828	17:16:38.36	−29:54:33.6	C	17.244	19.210	0.21367127	0.440	0.386	5000.04525
OGLE-BLG-ECL-000003	BLG616.03.6996	17:16:51.98	−29:04:29.1	NC	19.057	–	0.21434213	0.840	0.625	5000.14498
OGLE-BLG-ECL-000004	BLG616.10.93602	17:17:13.44	−28:38:07.1	NC	17.708	20.025	0.21488204	0.970	0.771	5000.03817
OGLE-BLG-ECL-000005	BLG617.19.15379	17:17:46.19	−29:32:42.2	NC	14.736	–	0.21549714	0.782	0.509	5000.18320
OGLE-BLG-ECL-000006	BLG616.26.30381	17:18:11.28	−27:58:02.9	NC	19.063	–	0.21877314	0.950	0.750	5000.10010
OGLE-BLG-ECL-000007	BLG616.01.26238	17:18:11.61	−28:59:37.3	NC	19.601	20.377	0.09176723	0.970	0.197	5000.03653
OGLE-BLG-ECL-000008	BLG615.11.36403	17:25:16.06	−30:05:26.2	NC	17.519	19.651	0.21770001	0.576	0.407	5000.16501
OGLE-BLG-ECL-000009	BLG612.25.57960	17:27:10.66	−27:43:57.5	NC	18.035	–	0.15077164	0.342	0.159	5000.00129
OGLE-BLG-ECL-000010	BLG613.07.75589	17:27:44.28	−29:46:16.1	NC	16.621	17.085	0.10051416	1.271	0.165	5000.01173
OGLE-BLG-ECL-000011	BLG662.21.5107	17:30:01.74	−30:24:29.8	NC	17.775	19.727	0.20005222	0.526	0.472	5000.03194
OGLE-BLG-ECL-000012	BLG613.18.38807	17:32:12.01	−29:05:16.4	NC	16.951	18.899	0.21894515	0.685	0.542	5000.11160
OGLE-BLG-ECL-000013	BLG654.14.22809	17:34:24.48	−29:51:38.8	NC	15.535	17.451	0.21386391	0.314	0.240	5000.13478
OGLE-BLG-ECL-000014	BLG621.29.94695	17:34:59.40	−21:45:07.2	NC	19.471	–	0.20875910	0.607	0.491	5000.04820
OGLE-BLG-ECL-000015	BLG654.05.20766	17:35:09.37	−30:12:44.8	C	18.173	20.495	0.20539043	0.877	0.860	5000.18653
OGLE-BLG-ECL-000016	BLG672.01.10260	17:35:24.66	−37:08:57.7	C	18.716	21.542	0.21272893	0.497	0.497	5000.21131
OGLE-BLG-ECL-000017	BLG680.25.40021	17:35:43.65	−37:09:58.4	C	19.327	21.625	0.21383009	0.728	0.609	5000.11979
OGLE-BLG-ECL-000018	BLG611.11.102686	17:36:09.08	−27:25:30.7	NC	18.338	21.161	0.17470363	0.132	0.091	5000.08124
OGLE-BLG-ECL-000019	BLG609.25.65430	17:36:30.19	−34:38:12.7	NC	19.427	–	0.16552070	0.371	0.369	5000.13526
OGLE-BLG-ECL-000020	BLG653.19.19121	17:37:14.38	−28:22:01.4	NC	18.228	21.775	0.14994447	0.461	0.362	5000.09106
OGLE-BLG-ECL-000021	BLG680.14.44506	17:37:22.60	−37:18:11.0	NC	19.360	21.754	0.21838043	0.987	0.774	5000.19109
OGLE-BLG-ECL-000022	BLG680.06.29442	17:37:49.48	−37:35:02.1	C	19.106	21.866	0.21921610	0.721	0.581	5000.02834
OGLE-BLG-ECL-000023	BLG611.09.16725	17:37:53.06	−27:17:40.9	NC	18.285	21.116	0.20038455	0.285	0.225	5000.02746
OGLE-BLG-ECL-000024	BLG609.06.71216	17:38:08.53	−35:13:25.4	NC	18.657	20.956	0.21938176	0.304	0.269	5000.07937
OGLE-BLG-ECL-000025	BLG611.17.72634	17:38:11.82	−27:06:05.2	NC	18.787	22.181	0.17295506	0.233	0.155	5000.16047
OGLE-BLG-ECL-000026	BLG625.15.81252	17:38:14.61	−22:56:53.7	C	18.893	21.104	0.21928025	0.313	0.299	5000.16745
OGLE-BLG-ECL-000027	BLG624.23.56697	17:39:02.10	−21:19:19.6	NC	18.378	21.117	0.17040292	0.207	0.194	5000.04398
OGLE-BLG-ECL-000028	BLG680.12.35846	17:39:03.54	−37:30:16.2	NC	18.862	–	0.18030005	0.719	0.567	5000.10937
OGLE-BLG-ECL-000029	BLG675.14.69526	17:39:26.25	−27:36:53.9	NC	17.129	17.950	0.20354910	0.342	0.319	5000.02214
OGLE-BLG-ECL-000030	BLG625.13.72702	17:39:35.38	−22:54:43.0	NC	19.029	–	0.14745975	0.211	0.183	5000.06232

The vast majority of the binary systems in our sample are new detections. Only several objects were already known from other investigations, mostly from the previous stages of the OGLE project. OGLE-BLG-ECL-000142 is the mentioned OGLE BW3 V38 (Udalski *et al.* 1995, Maceroni and Rucinski 1997). Unfortunately, in the OGLE-IV field this star fell in a gap between two CCD chips of the mosaic camera, and we can provide only the OGLE-III photometry of this object. OGLE-BLG-ECL-000163 (= OGLE BUL-SC16 335) was discovered by Połubek *et al.* (2007) and classified as an HW Vir-type binary – system consisting of a B-type subdwarf (sdB) and a cool main-sequence star (Wood *et al.* 1993). The spectroscopic analysis performed by Geier *et al.* (2014) confirmed that the primary component is an sdB ($T_{\rm eff} = 31\,500 \pm 1800$ K, $\log g = 5.7 \pm 0.2$) and the secondary is an M dwarf with the mass of $0.16 \pm 0.05\ M_{\odot}$. OGLE-BLG-ECL-000115 (= OGLE-I BW9 189794) was identified by Szymański *et al.* (2001) and included in their catalog of contact binaries. OGLE-BLG-ECL-000009 and OGLE-BLG-ECL-000045 are central stars of planetary nebulae Th 3-15 and Pe 1-9, respectively. The latter object was identified by Miszalski *et al.* (2009). The positions of four eclipsing binaries: OGLE-BLG-ECL-000056, OGLE-BLG-ECL-000126, OGLE-BLG-ECL-000131, and OGLE-BLG-ECL-000201, coincide with Novae: V825 Sco, V4742 Sgr, Nova Sgr 1986, and V5116 Sgr, respectively.

Fig. 1 shows the positions of our binary systems in the sky. Most of the objects are likely located in front of the Galactic bulge. Note that we detected a number of binary stars in the heavily reddened regions around the Galactic plane ($|b| < 1$). In these regions stars from the Galactic bulge (for example RR Lyr variables, Soszyński *et al.* 2014) are completely obscured in the visual bands by the interstellar matter.

Color–magnitude diagram for our sample is shown in Fig. 2. The apparent $(V-I)$ colors of individual objects are dominated by the interstellar reddening, which depends on the position in the sky and the distance to a star, which causes that various types of binary systems span a wide range of colors. The only exceptions are binary systems exhibiting significant reflection effect (Section 5.3), which almost without exception are blue. In Fig. 3, we present distributions of the orbital periods for the entire sample and separately for different types of binary systems.

5. Results

5.1. M-dwarf Binaries and OGLE-BLG-ECL-000066

A strong distortion of one or both components is distinctly visible in 161 light curves. 75 of them have similar depths of the primary and secondary minima and these stars are classified as candidates for contact binaries. The status of these objects has to be confirmed spectroscopically. The shortest-period light curves of our candidates for W UMa stars are displayed in Fig. 4. The most compact binaries in this group have $P < 0.19$ d, which, if confirmed, would slightly shift the short-

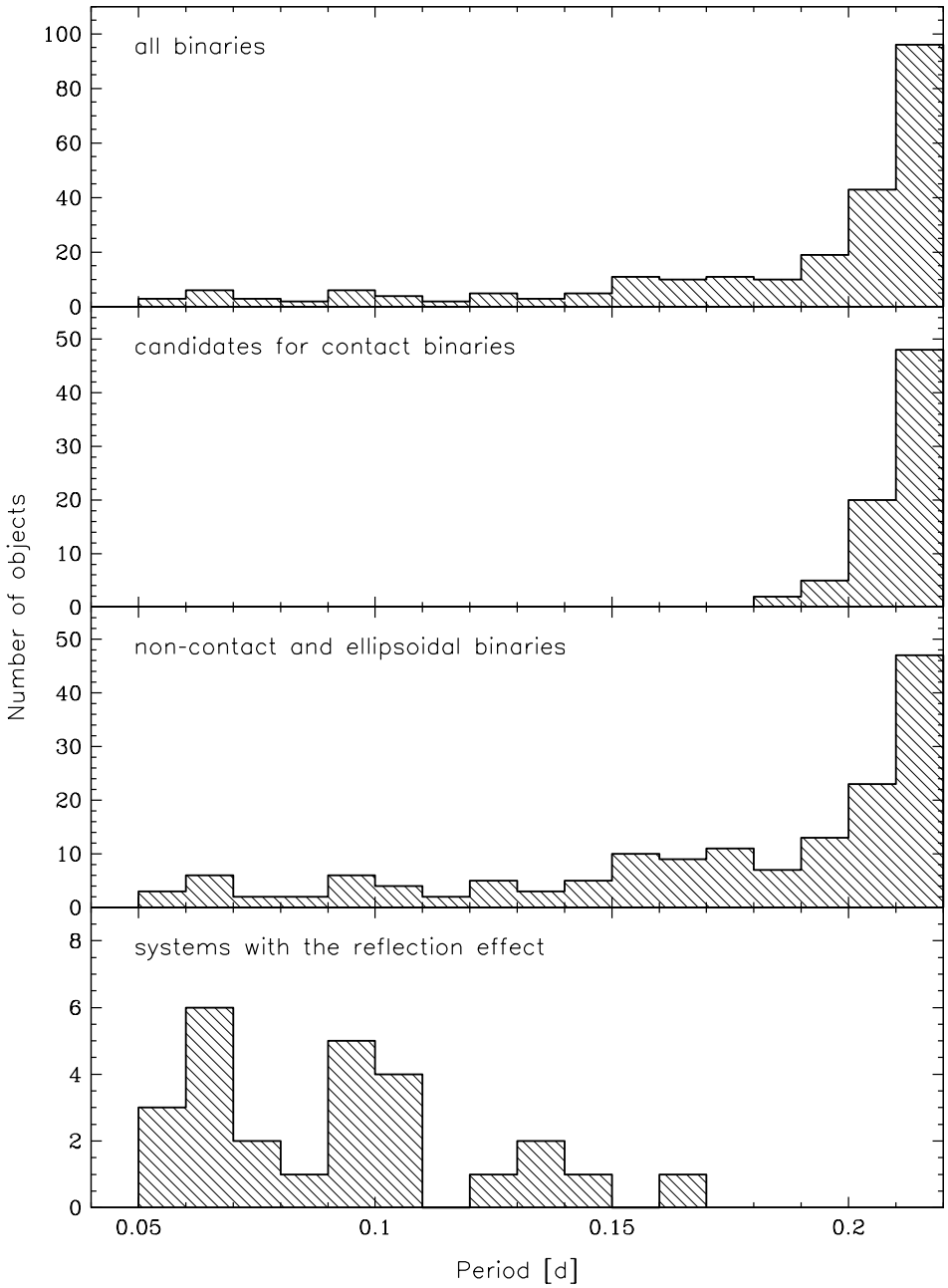

Fig. 3. Orbital period distribution of the ultra-short-period binary systems. The consecutive panels show the period distribution of the whole sample, the candidates for contact binary systems, non-contact binaries and the sub-sample of eclipsing binaries with a strong reflection effect.

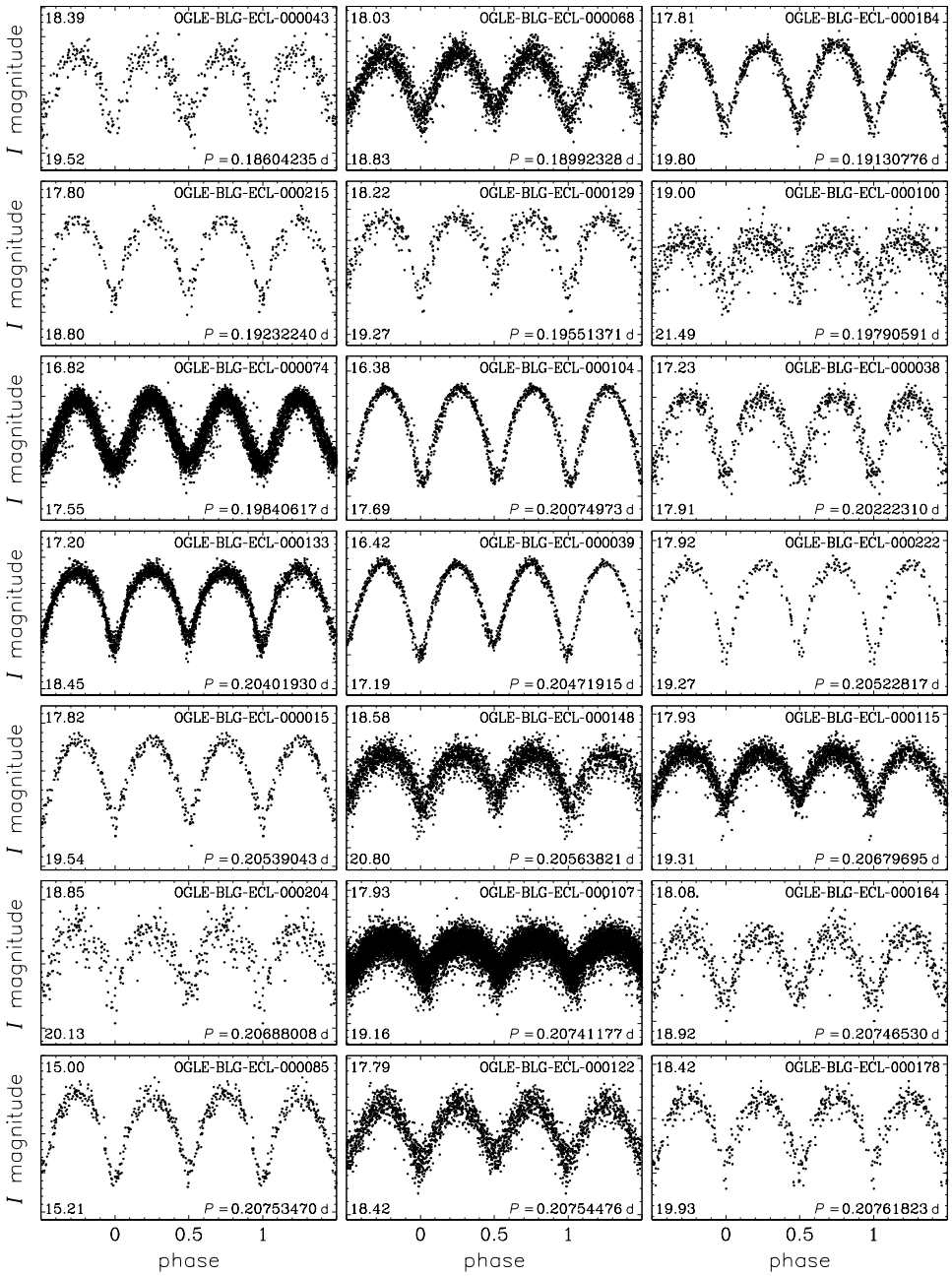

Fig. 4. *I*-band light curves of the shortest-period candidates for contact binary systems. The light curves are arranged according to the orbital periods.

period cut-off for W UMa stars, but still this limit is much longer than for other types of binary systems.

Our sample also contains several possible M-dwarf binaries in the detached or semi-detached configuration with periods much below this limit. OGLE-BLG-ECL-000066 has period shorter than any known main-sequence binaries: 0.0984 d. Its light curve (Fig. 5) resembles those of OGLE BW3 V38 (Maceroni and Rucinski 1997) and GSC 2314-0530 (Dimitrov and Kjurkchieva 2010), which are M-dwarf binary systems in near-contact configuration.

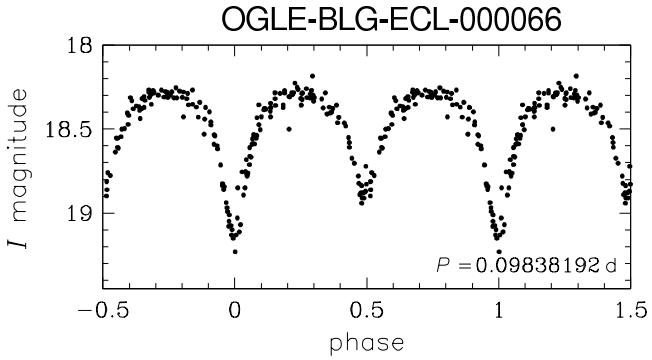

Fig. 5. *I*-band light curves of OGLE-BLG-ECL-000066 – candidate for the shortest-period known binary consisting of main sequence stars.

The full orbital solution for this system will be possible with the spectroscopic measurements, although we are aware that this would be a difficult task, since the target is faint and heavily reddened. Moreover, its short orbital period prevents exposures longer than about 15 minutes, because of the motion blur of the spectral lines. Nevertheless, such observations should be feasible with modern spectrographs attached to large telescopes like X-shooter or FORS at VLT.

However, even without spectroscopic measurements we can still constrain the absolute parameters of the system components and attempt to reproduce the evolutionary history of the binary. The first constraint results from the depths of the minima. They are equal to 0.86 and 0.62 mag, suggesting that the orbit inclination $i \approx 90^{\rm o}$ and the difference in brightness of the components is of the order of 20%, hence the difference in mass is only about 5%, *i.e.*, masses are almost equal. Another constrain is connected with a low value of the orbital period $P_{\rm orb}$. Assuming that both components are equal mass dwarfs nearly filling their Roche lobes we have

$$P_{\rm orb} > P_{\rm crit} = 0.174\sqrt{\frac{R^3}{M}} \qquad (1)$$

where R and M are radius and mass of each component in solar units and $P_{\rm crit}$ is the critical period in days, when both components just fill their Roche lobes. The observed radii of low-mass stars are approximately equal to their masses, if both are expressed in solar units (Torres *et al.* 2010). Adopting this relation we obtain

$P_{\rm crit} \approx 0.350R$ and $R < 2.857P_{\rm orb}$. For OGLE-BLG-ECL-000066 the resulting limit for radius of each component is $R < 0.28R_\odot$, equivalent to $M < 0.28M_\odot$. The corresponding spectral type must be later than M3.5 (Lang 1992) but not later than M5 if the components almost fill their Roche lobes. We adopt M4 type for both components.

These estimates are confirmed by the WD code (Wilson and Devinney 1971) fitted to the *I*-band light curve. Assuming two M4-type components, the model gives masses $M_1 = 0.22M_\odot$ and $M_2 = 0.21M_\odot$, and the mass ratio $q = 0.95$. The radii of both components are $R_1 = 0.26R_\odot$ and $R_2 = 0.23R_\odot$ and the inclination of the orbit $i = 86^{\rm o}$. In such a configuration, the primary component is very close to fill its Roche lobe.

The last constraint can be derived from photometry of the variable: $V_{\rm max} = 21.5$, $I_{\rm max} = 18.285$, $J = 16.47$, $H = 15.69$, and $K = 15.09$, all in magnitudes. The *V*-band observations are at the faint-end magnitude limit of the OGLE survey and are uncertain within ~ 0.5 mag. The near-infrared *JHK* magnitudes were obtained by the VISTA Variables in the Via Lactea (VVV) survey (Minniti *et al.* 2010). The epochs of these observations fell outside the eclipses, close to the maximum light. OGLE-BLG-ECL-000066 is located only 0.5 degrees from the Galactic plane, thus its apparent luminosity must be severely affected by the interstellar extinction. Indeed, its $(V-I)$ apparent color index is one of the largest in our sample (Fig. 2).

We will estimate the amount of interstellar absorption toward our target using its near-infrared measurements. It is known that dwarfs in the range of spectral types from M1 to M5 have nearly the same intrinsic $(J-H)$ color: 0.64 ± 0.02 mag (Bessell and Brett 1988). This gives immediately the near-infrared color excess to OGLE-BLG-ECL-000066 of $E(J-H) = 0.14$ mag. It is known that the interstellar extinction toward the Galactic bulge is anomalous (*e.g.*, Udalski 2003b, Nataf *et al.* 2013), but this affects mostly the optical passbands. In the near-infrared we can use in the first approximation the standard reddening law (Schlegel *et al.* 1998): $E(J-K) = 1.62E(J-H) = 0.23$ mag. This gives the dereddened $(J-K)$ index of OGLE-BLG-ECL-000066 equal to 1.15 mag, which agrees well with the range of this index observed for nearby M4 stars (Riaz *et al.* 2006).

In the optical domain, the anomalous extinction in the Galactic bulge makes dereddening very uncertain. The standard reddening law (Schlegel *et al.* 1998) can be used to estimate an upper limit for the amount of interstellar extinction: $A_I = 5.88E(J-H) \leq 0.82$ mag and $A_V = 10.05E(J-H) \leq 1.41$ mag. This implies that the intrinsic $(V-I)$ color of OGLE-BLG-ECL-000066 is larger than 2.6 mag, which according to Bessell and Brett (1988) corresponds to dwarfs later than M3.5 and earlier than M5 (assuming no extinction). This result is fully consistent with our previous estimates.

Now we can reconstruct the evolutionary history of the binary orbit. We assume that the only mechanism influencing the orbit evolution of OGLE-BLG-ECL-

000066 has been mass and angular momentum loss (AML) due to the magnetized winds from both components. Rates for both processes are taken from the model described by Stępień (2006a, 2011), and Gazeas and Stępień (2008).

$$\dot{M} = -10^{-11} R^2 \,, \tag{2}$$

$$\frac{\mathrm{d}H}{\mathrm{d}t} = -9.8 \times 10^{41} R^2 M/P \,. \tag{3}$$

Here H is the binary angular momentum (AM) in cgs units and we assume again equal mass components. The formulae apply to binaries in the so called saturation regime when the stellar rotation period (equal in this case to orbital period) is shorter than $\sim 3-4$ d (Randich *et al.* 1996).

Fig. 6 presents the time evolution of the orbital period for two binaries with initial component masses equal to $0.22 M_{\odot}$ (solid line) and $0.24 M_{\odot}$ (dotted line), and the initial periods between 0.3-0.7 d. Due to the wind, each star loses about 2-4% of its original mass, before the orbital period reaches the value observed for OGLE-BLG-ECL-000066 (dashed horizontal line). End of each solid/dotted line marks the moment when the binary fills the Roche lobe, or the Universe age is reached, whichever comes first. As we see, the initial period of OGLE-BLG-ECL-000066 must have been shorter than 0.6 d, or, if its age is lower than 10 Gyr as can be judged from its position within a thin Galactic disk, shorter than 0.4 d.

Our results demonstrated the existence of an ultra-short-period population of near contact binaries with M-type components and periods close to, or even below 0.1 d. Angular momentum loss is insufficient during the Hubble time to reduce an initial period of 1.5 d to the observed values. The adopted formulae are extrapolated for low-mass stars from data on more massive stars. Can this extrapolation be incorrect and the angular momentum loss rate is in fact substantially higher, as suggested e.g. by Jiang *et al.* (2012)? We calculated several evolutionary models of binaries with initial component masses equal to 0.24 $M_{\odot}$ and AML rate increased arbitrarily by a factor of 5 and 10. Binaries with the initial period of 1.5 d reach the value observed for OGLE-BLG-ECL-000066 in 6.6 and 3.26 Gyr, respectively. Even binaries with the initial period of 2.5 d reach this value within the Hubble time. However, the AML rate of single M stars does not seem to be so high. In fact, the analysis of rotation of M-type stars by Delfosse *et al.* (1998) indicates that the time scale for spin-down of single stars increases with the decreasing mass from 50 Myr for G dwarfs to a few Gyr for M3-M4 stars. The same ratio of both time scales can be obtained from Eq. 3. Barnes and Kim (2010) derived an empirical expression for the AML rate of cool stars with different masses. The rate is proportional to the ratio of stellar moment of inertia and a parameter called turnover time. This ratio decreases by a factor of $\sim 10^2$ between 1 and 0.2 solar mass star with no sign of increase for low mass stars. So, the substantially increased AML rate of M-type stars during the main sequence evolutionary phase finds no substantiation.

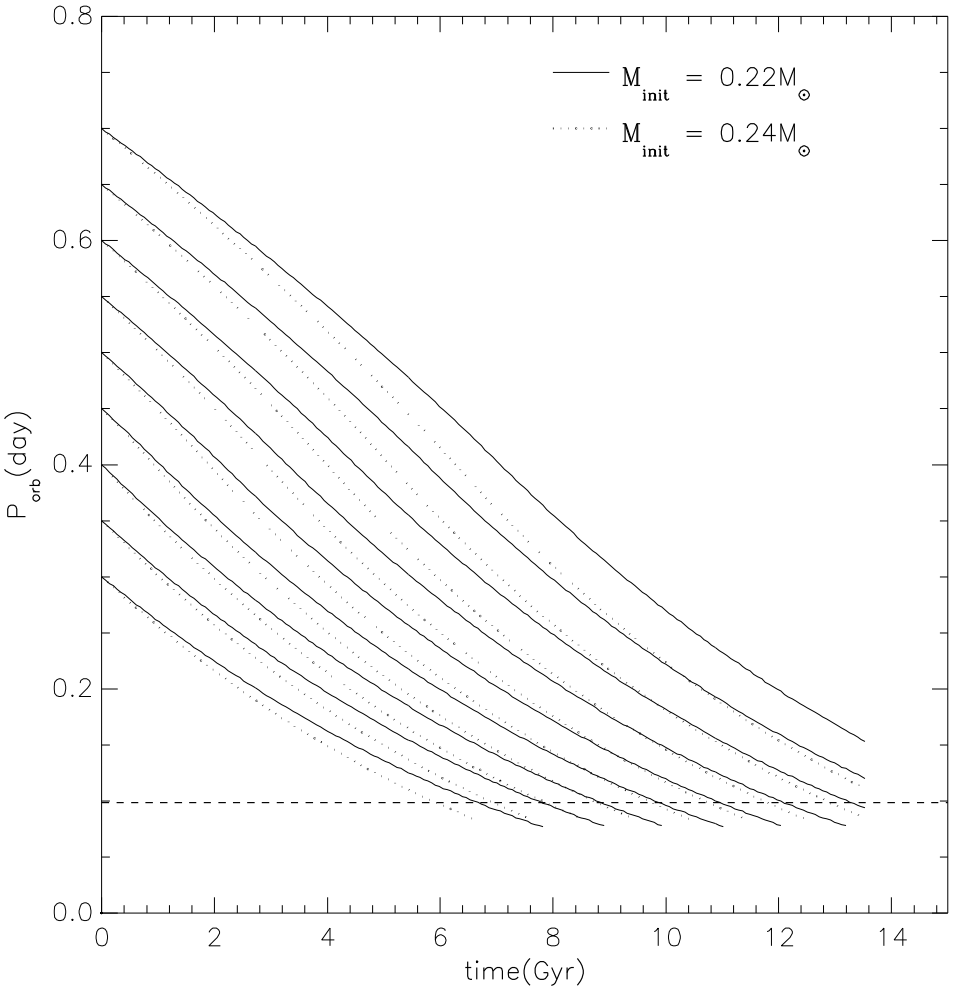

Fig. 6. Orbital period evolution of two binaries with equal mass components and different initial periods. Solid line corresponds to a binary with initial component masses equal to 0.22 $M_\odot$ and a dotted line to a binary with masses equal to 0.24 $M_\odot$. A horizontal dashed line marks the period of OGLE-BLG-ECL-000066.

Another possibility is that M-stars lose a substantial fraction of their AM during the T Tau phase. The life-time of a cool star in this phase is roughly equal to 1% of the main sequence life time. For solar type stars it amounts to only about 10^7–10^8 years – short enough to neglect the shortening of the orbital period even if AML rate in T Tau phase for a single star is significantly higher than in the main sequence phase. This may not be true, however, for binaries with component masses 0.2–0.3 $M_\odot$ which spend ~ 1 Gyr before they reach the zero age main sequence. Little is known about activity of low mass T Tau stars and their interaction with circumstellar (or circumbinary) disks so we cannot exclude this possibility. Observations of young M-type binaries would help to follow the period evolution in the early evolutionary phases.

Alternatively, we can consider dynamical interaction with other stars. Naoz and Fabrycky (2014) computed orbit evolution of a numerous sample of binaries under the influence of the KCTF mechanism, including relativistic effects and so called octupole-level approximation. The resulting period distribution of the inner binaries contains a fraction of periods shorter than 1 d. A majority of them originate from binaries with equally short initial periods because the authors adopted the initial period distribution after Duquennoy and Mayor (1991), which extends smoothly to zero. By adopting a cut-off period of 1.5-2 d we should reject these binaries as nonphysical but a very limited number of longer period binaries also evolved to, or below 1 d limit (see their Fig. 3). We conclude that the KCTF mechanism can produce binaries with periods of 1 d or less under very exceptional circumstances. Based on simple statistics, Drake *et al.* (2014) argue that dM+dM ulta-short-period binaries are indeed extremely rare among photometrically variable stars. To verify this hypothesis the bias-free period distribution of cool binaries should be obtained.

5.2. Period changes

The detection of period changes in close binary systems would be a powerful test for models explaining the short-period cut-off in contact binaries. Generally, the orbital periods should decrease over time, as the systems lose angular momentum from magnetic braking, which ultimately leads to the coalescence. So far the only stellar merger observed before and during the act of coalescence was V1309 Sco (Tylenda *et al.* 2011), photometrically monitored by the OGLE survey.

Kubiak *et al.* (2006) detected statistically significant secular period changes in 134 of 669 analyzed contact binaries observed by OGLE toward the Galactic bulge (Szymański *et al.* 2001). The distribution of the rates of the period changes occurred to be nearly symmetrical around zero. Pilecki *et al.* (2007) analyzed 1711 contact and semi-detached binaries observed by the ASAS project and found 31 period-changing systems – 21 decreasing and 10 increasing periods. Lohr *et al.* (2013) found statistically significant (3σ) period changes in 38 of 143 short-period binaries observed by the SuperWASP project. The distribution of the period-change rates was approximately symmetrical around zero.

We used the fitted model light curves to perform the analysis of the orbital period changes for all eclipsing binaries in our sample, although reliable results can be obtained only for the stars that were observed during both – OGLE-III and OGLE-IV – stages of the survey. Other light curves have too short time span to draw statistically significant conclusions from the $(O-C)$ diagrams. Our procedure was as follows: each light curve was divided into different observing seasons (spanning one year of observations), and for each such chunk we shifted the phase of the model light curve to minimize the sum of squared differences between the observed and the model light curve. In such a way we obtained $(O-C)$ diagrams for our stars with one point per every observing season.

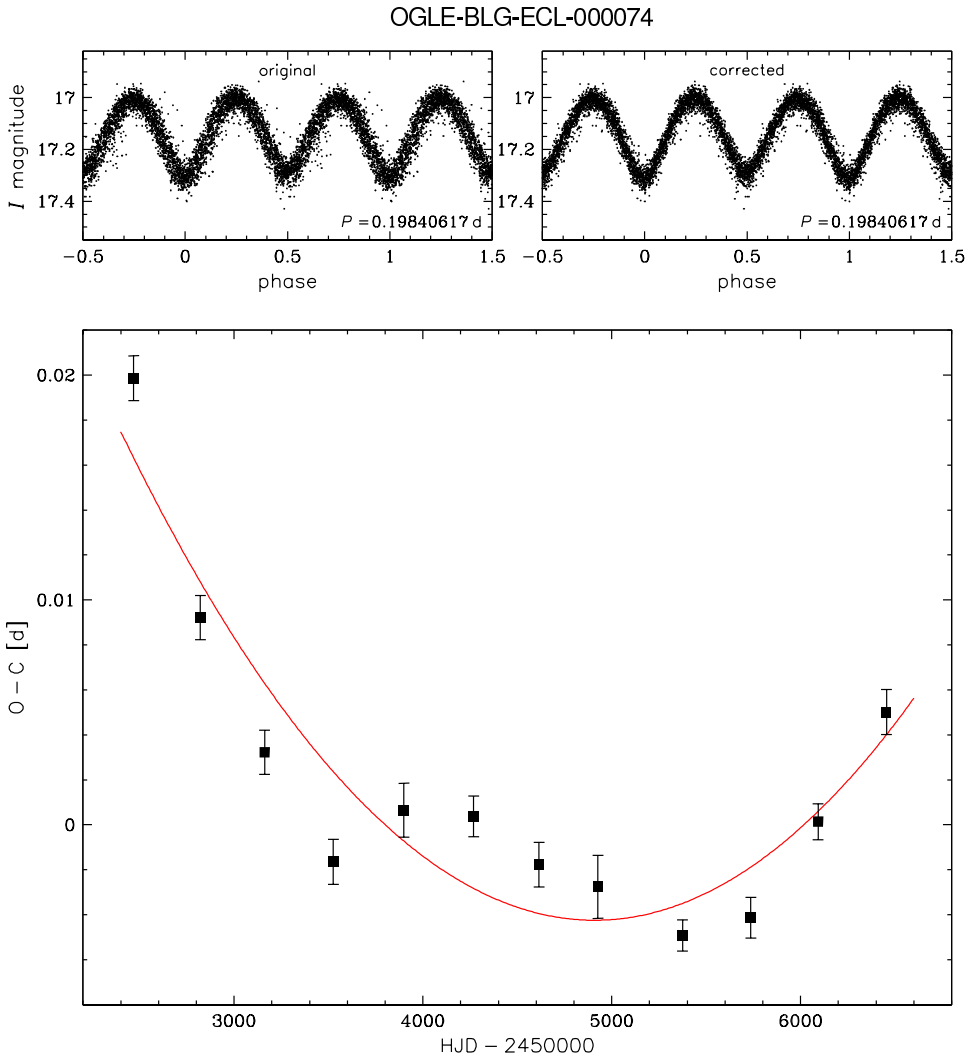

Fig. 7. *Upper panels*: light curve of a compact binary system OGLE-BLG-ECL-000074. *Left panel* presents the original data folded with the mean orbital period, while *right panel* presents the light curve corrected for the monotonic period increase measured in the $(O-C)$ diagram (*lower panel*).

Among 78 binary systems observed by OGLE over 12 or more years, we found 16 objects of which orbital periods seem to be unstable. In 10 cases the changes of periods are roughly monotonic, like in the case of OGLE-BLG-ECL-000074 shown in Fig. 7. Table 2 lists the binary systems with secular period changes. Seven systems increase and three systems decrease their orbital periods. Most of these objects are candidates for contact or nearly contact binary systems. The shortest-period binary changing its period is OGLE-BLG-ECL-000131 = Nova Sgr 1986. In six systems listed in Table 3, the orbital period changes are likely not constant. Since the typical time scales of the period variations are of the order of several years, in most cases we cannot unambiguously distinguish whether these variations

T a b l e 2

Eclipsing binary systems with monotonic period changes.

Identifier	Type	$P_{\rm orb}$ [d]	$\mathrm{d}P_{\rm orb}/\mathrm{d}t$ [s/year]
OGLE-BLG-ECL-000065	C	0.21221016	−0.04
OGLE-BLG-ECL-000073	C	0.21831428	0.17
OGLE-BLG-ECL-000074	C	0.19840617	0.22
OGLE-BLG-ECL-000131	NC	0.15356160	0.29
OGLE-BLG-ECL-000141	C	0.21436650	−0.13
OGLE-BLG-ECL-000144	C	0.21894593	0.17
OGLE-BLG-ECL-000145	C	0.21104030	0.10
OGLE-BLG-ECL-000148	C	0.20563821	0.14
OGLE-BLG-ECL-000168	NC	0.20280139	−0.15
OGLE-BLG-ECL-000173	NC	0.21373651	0.38

are strictly periodic or they are irregular in nature. Cyclic period variations may reveal the presence of an unseen tertiary companion due to the light travel time effect. Irregular period fluctuations may be caused by non-stationary mass transfer within the system or by mass ejections from the system. Table 3 gives possible lengths of the period change cycles.

T a b l e 3

Eclipsing binary systems with cyclic or irregular period changes.

Identifier	Type	$P_{\rm orb}$ [d]	$P_{\rm cycle}$ [d]
OGLE-BLG-ECL-000069	NC	0.19272500	2300
OGLE-BLG-ECL-000104	C	0.20074973	1400
OGLE-BLG-ECL-000107	C	0.20741177	2400
OGLE-BLG-ECL-000127	NC	0.16641697	1500
OGLE-BLG-ECL-000170	C	0.21491916	3300
OGLE-BLG-ELL-000015	ELL	0.21996525	2200

5.3. Eclipsing Binaries with a Strong Reflection Effect

Among detached eclipsing binary systems, 26 objects constitute a homogeneous group. The light curves of 21 shortest-period objects from this group are shown in Fig. 8. These stars are characterized by narrow eclipses with very different depths of the primary and secondary eclipses and by the sinusoidal modulation between the eclipses caused by the reflection of light received by the cooler star from the hotter component. Ten similar systems were recently reported in the OGLE-III Galactic disk fields (Pietrukowicz *et al.* 2013), six of which have orbital periods shorter than 0.15 d. Objects presented in Fig. 8 belong to the bluest

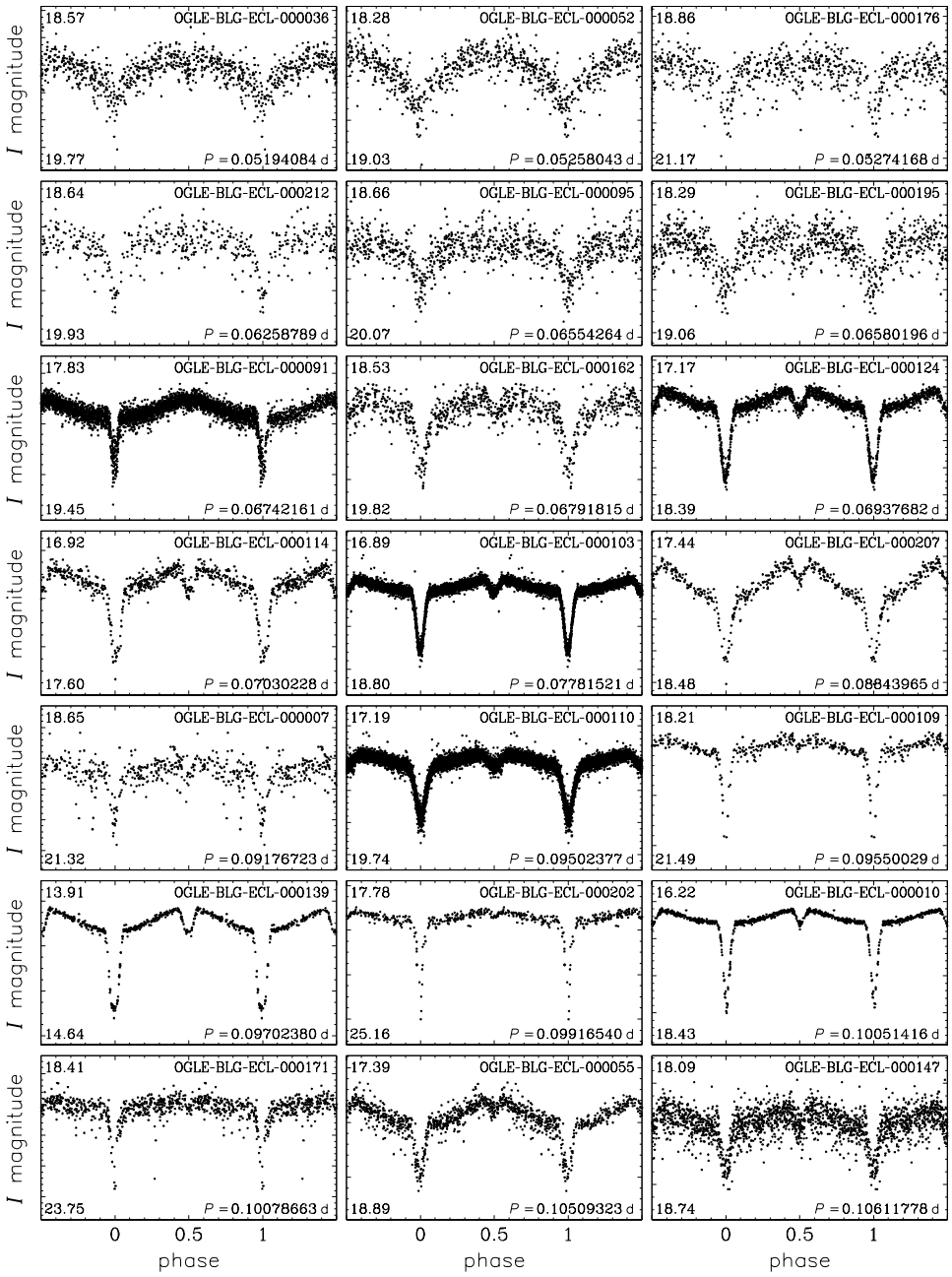

Fig. 8. *I*-band light curves of the shortest-period eclipsing binary systems with a strong reflection effect. The light curves are arranged according to the increasing orbital periods.

and the shortest-period binary systems in our collection (see Fig. 2 and the lower panel of Fig. 3). These systems consist likely of a cool main sequence star and a hot evolved remnant: an sdB or a white dwarf (*e.g.*, İbanoğlu *et al.* 2004, Zorotovic and Schreiber 2013). Their short periods suggest that they are post common-envelope systems (Paczyński 1976), so they are important for understanding common envelope evolution and subsequent system behaviors. Due to their well-defined, deep primary eclipses and short orbital periods, such objects have also great potential in detecting circumbinary substellar companions. At least a dozen compact binaries containing a white dwarf or an sdB primary have been claimed to host a planetary or brown dwarf third companion from the eclipse timing measurements (*e.g.*, Guinan and Ribas 2001, Lee *et al.* 2009, Beuermann *et al.* 2010), however the reality of some of these detections is controversial (Lohr *et al.* 2014). Our preliminary timing analysis showed no plausible evidence for period changes in any binary system with a strong reflection effect.

5.4. Cataclysmic Variables

Cataclysmic variables (CVs) are interacting binary systems consisting of a white dwarf and a mass transferring secondary (donor), usually a low-mass main-sequence star. If the magnetic field of the white dwarf is weak, the gas flowing through the inner Lagrangian point forms an accretion disk around the primary. The location where the material hits the edge of a disk is called the hot spot. In dwarf novae, instabilities in the disk lead to regular outbursts with typical amplitudes of 2–5 mag.

About 20% of known CVs are eclipsing binaries (Warner 1995). An analysis of a complex eclipse shape may provide information about the relative brightness, sizes and masses of both components and the hot spot (*e.g.*, Wood *et al.* 1986, Horne *et al.* 1994). The distribution of orbital periods reflects the evolution of CVs.

Our sample contains five eclipsing dwarf novae. Their unfolded and folded light curves are showed in Fig. 9. OGLE-BLG-ECL-000082 (with the orbital period of 1.726 h) probably belongs to SU UMa-type dwarf novae with brighter and longer superoutbursts every ~ 420 d. There are only a handful of eclipsing SU UMa stars known. Analysis of their light curves may give evidence for the origin of superoutbursts (*e.g.*, Smak 1994, Bąkowska and Olech 2014). The remaining four objects have orbital periods longer than 4 h. They are likely members of the U Gem class. The outbursts have various amplitudes and recurrence intervals, while the eclipses are always deep, exceeding 0.85 mag in the I-band, but with no clear reflection effect.

Ten further detached eclipsing systems exhibit similar depths of minima (in some cases exceeding 2 mag), but with no outbursts (Fig. 10). Secondary eclipses are very shallow, sometimes invisible, and distinct reflection effect is absent. Some of these objects show irregular variations outside the eclipses (flickering), produced by the inner disk and/or the hot spot. These are probably UX UMa-type stars,

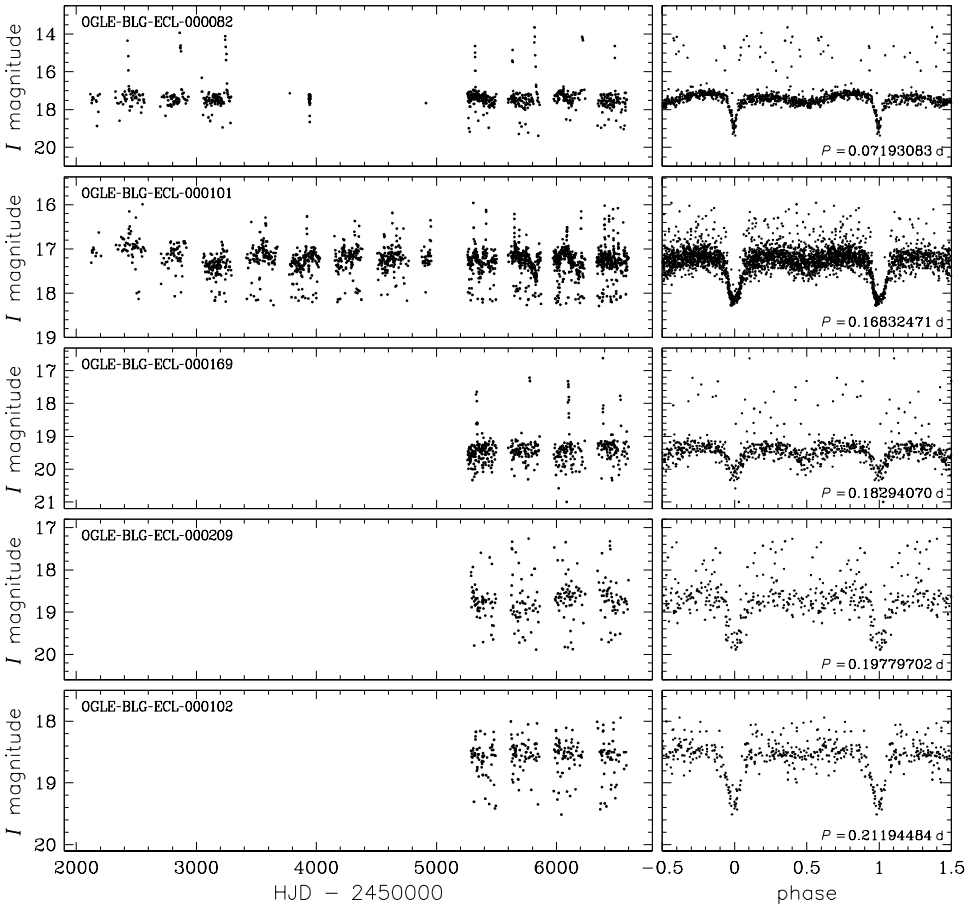

Fig. 9. *I*-band light curves of dwarf novae in our sample. *Left panels* present unfolded light curves, *right panels* show the same light curves folded with the orbital periods.

i.e., Nova and Nova-like cataclysmic variables (*e.g.*, Smak 1994). Spectroscopic observations would provide conclusive evidence about the nature of the remaining objects.

5.5. The Case of OGLE-BLG-ECL-000034

The most bizarre light curve in our collection is shown by OGLE-BLG-ECL-000034 (Fig. 11). Deep eclipses ($\Delta I = 1.1$ mag) recur every 3.777 h. The out-of-eclipse brightness is variable. Between phases 0.25 and 0.8 the light curve has sinusoidal shape, while between 0.8 and 0.9 (0.15 and 0.25) we observe steep brightening (fading). The light curve is almost symmetric. The ephemeris for the mid-eclipse are:

$$\mathrm{HJD}_{\mathrm{eclipse}} = 2\,455\,000.082(1) + 0.15737024(4) \cdot E\,.$$

The observed changes could be explained, if OGLE-BLG-ECL-000034 were a high inclination polar. Polars (AM Her-type stars) are cataclysmic variables in

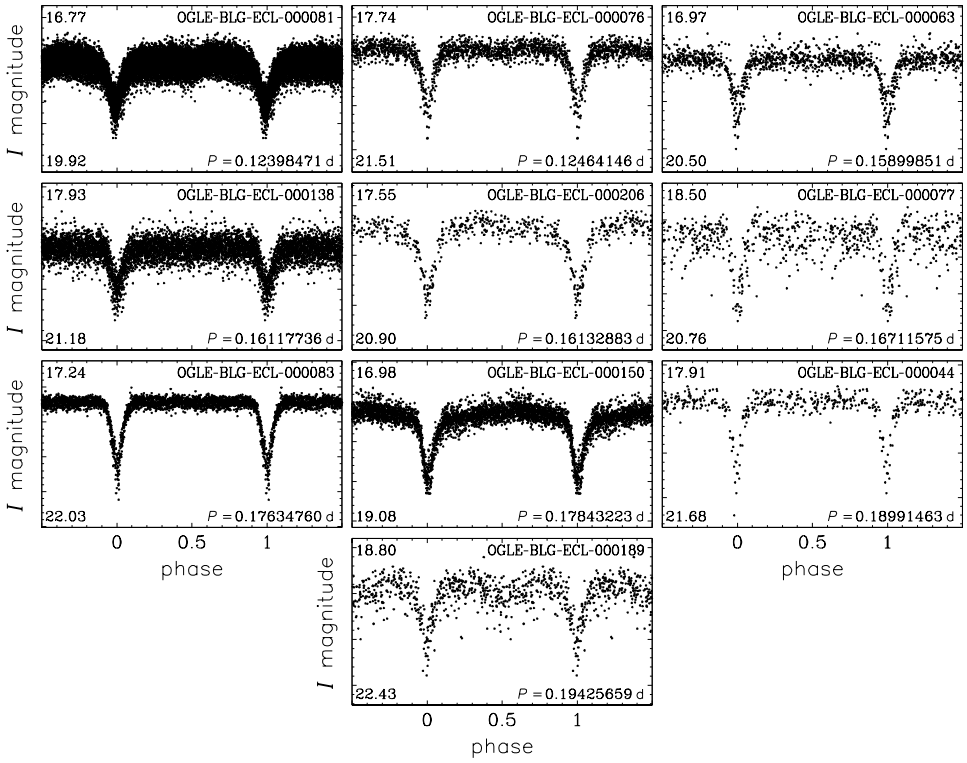

Fig. 10. *I*-band light curves of candidates for cataclysmic variables.

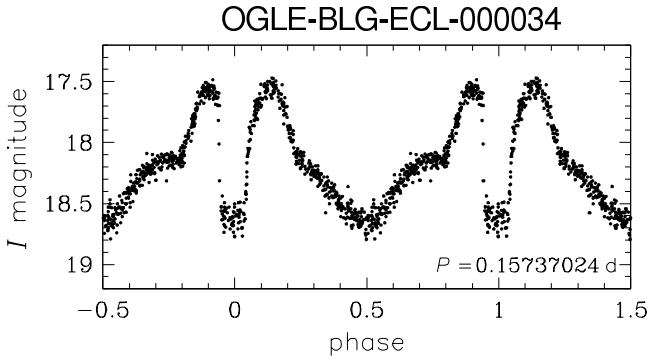

Fig. 11. *I*-band light curve of OGLE-BLG-ECL-000034 – a candidate for a high inclination polar.

which the magnetic field of the white dwarf is very strong ($B > 10^3$ T at the surface). The accretion disk cannot be formed and the material from the secondary follows magnetic field lines, heading toward magnetic pole(s). Accretion regions around magnetic pole(s) are main sources of the radiation from the system. The strong magnetic field also synchronize the rotation of the white dwarf and the binary.

To account for the light curve properties, the inclination of the system has to be very high and the magnetic axis of the white dwarf must point toward the secondary. In such a case, the gas flows preferentially onto the closer magnetic pole. This pole

is hidden behind the white dwarf between phases 0.25 and 0.8. Bumps between 0.8 and 0.25 can be naturally explained by the emergence of the accretion region. It is a source of cyclotron radiation; possibly, a cyclotron hump peaks around 800 nm, giving rise to the large amplitude in the I-band. The light curve of the well-known polar, EP Dra, shows similar features (see Remillard *et al.* 1991 and their Fig. 6). The red dwarf secondary, filling its Roche lobe, is strongly distorted, producing an additional sinusoidal signal at half of the orbital period.

We are able to assess basic system parameters from the light curve examination. Assuming that the secondary fills its Roche lobe and it follows the standard mass-radius relation for red dwarfs, a mass of the secondary is $M_2 \approx 0.065 P_{\rm orb}^{5/4}\ M_\odot = 0.34\ M_\odot$ (Hellier 2001). The eclipse width is $\Delta\varphi \approx 0.1$, suggesting a relatively high mass ratio $q \gtrsim 0.5$ (Horne 1985). For the inclination $i = 85^\circ$, the white dwarf mass is $M_1 \approx 0.6\ M_\odot$ and the binary separation $a \approx 1.2\ R_\odot$. Lower inclination, $i = 80^\circ$, corresponds to the less massive white dwarf $M_1 \approx 0.4\ M_\odot$ and slightly smaller separation $a \approx 1.1\ R_\odot$.

We checked that there is no X-ray counterpart to this source in the HEASARC[‡] database. Further spectroscopic and polarimetric observations are needed to testify our hypothesis.

6. Conclusions

We presented a sample of 242 ultra-short-period binary systems detected toward the Galactic bulge by the OGLE survey. Our collection significantly increases the number of known binary systems with periods below 0.22 d. Together with the list of objects we provide their long-term time-series photometry in two filters. The sample is very heterogeneous – it contains candidates for contact binaries, semi-detached and detached systems, dwarf novae, and HW Vir stars. One of our objects – OGLE-BLG-ECL-000066 – is a candidate for the shortest-period known binary with non-degenerate components. The existence of such systems is a challenge for the binary evolution theory.

The presented sample is a forerunner of the OGLE collection of eclipsing and ellipsoidal binary systems toward the Galactic bulge which will be published in the future. Binary stars with the orbital periods above the adopted limit – 0.22 d – are among the most numerous variable stars. We expect that the total number of eclipsing stars in the OGLE collection should exceed one hundred thousand.

Acknowledgements. We are grateful to Z. Kołaczkowski and A. Schwarzenberg-Czerny for providing software which enabled us to prepare this study.

The OGLE project has received funding from the European Research Council under the European Community's Seventh Framework Programme (FP7/2007-2013)/ERC grant agreement no. 246678 to AU. This work has been supported by

[‡]http://heasarc.gsfc.nasa.gov

the Polish National Science Centre grant No. DEC-2011/03/B/ST9/02573. We gratefully acknowledge financial support from the Polish Ministry of Science and Higher Education through the program “Ideas Plus” award No. IdP2012 000162.

REFERENCES

Alard, C., and Lupton, R.H. 1998, *ApJ*, **503**, 325.
Bąkowska, K., and Olech, A. 2014, *Acta Astron.*, **64**, 247.
Barnes, S.A., and Kim, Y.-C. 2010, *ApJ*, **721**, 675.
Bessell, M.S., and Brett, J.M. 1988, *PASP*, **100**, 1134.
Beuermann, K., Hessman, F.V., Dreizler, S., *et al.* 2010, *A&A*, **521**, L60.
Bonnell, I.A. 1994, *MNRAS*, **269**, 837.
Delfosse, X., Forville, T., Perrier, C., and Mayor, M. 1998, *A&A*, **331**, 581.
Dimitrov, D.P., and Kjurkchieva, D.P. 2010, *MNRAS*, **406**, 2559.
Drake, A.J., Djorgovski, S.G., García-Álvarez, D., *et al.* 2014, *ApJ*, **790**, 157.
Duquennoy, A., and Mayor, M. 1991, *A&A*, **248**, 485.
Fabrycky, D., and Tremaine, S. 2007, *ApJ*, **669**, 1298.
Gazeas, K., and Stępień, K. 2008, *MNRAS*, **390**, 1577.
Geier, S., Østensen, R.H., Heber, U., *et al.* 2014, *A&A*, **562**, A95.
Guinan, E.F., and Ribas, I. 2001, *ApJ*, **546**, L43.
Hellier, C. 2001, Cataclysmic Variable Stars: How and Why they Vary (New York: Springer Verlag).
Horne, K. 1985, *MNRAS*, **213**, 129.
Horne, K., Marsh, T.R., Cheng, F.H., Hubeny, I., and Lanz, T. 1994, *ApJ*, **426**, 294.
Hypki, A., and Giersz, M. 2013, *MNRAS*, **429**, 1221.
İbanoğlu, C., Çakırlı, Ö., Taş, G., and Evren, S. 2004, *A&A*, **414**, 1043.
Jiang, D., Han, Z., Ge, H., Yang, L., and Li, L. 2012, *MNRAS*, **421**, 2769.
Kratter, K.M., Matzner, C.D., Krumholz, M.R., and Klein, R.I. 2010, *ApJ*, **708**, 1585.
Kubiak, M., Udalski, A., and Szymanski, M.K. 2006, *Acta Astron.*, **56**, 253.
Lang, K. R. 1992, Astrophysical Data. Planets and Stars (Berlin: Springer).
Lee, J.W., Kim, S.-L., Kim, C.-H., Koch, R.H., Lee, C.-U., Kim, H.-I., and Park, J.-H. 2009, *AJ*, **137**, 3181.
Lohr, M.E., Norton, A.J., Kolb, U.C., Maxted, P.F.L., Todd, I., and West, R.G. 2013, *A&A*, **549**, A86.
Lohr, M.E., Norton, A.J., Anderson, D.R., *et al.* 2014, *A&A*, **566**, A128.
Maceroni, C., and Rucinski, S.M. 1997, *PASP*, **109**, 782.
Machida, M.N., Tomisaka, K., Matsumoto, T., and Inutsuka, S. 2008, *ApJ*, **677**, 327.
Minniti, D., Lucas, P.W., Emerson, J.P., *et al.* 2010, *New Astronomy*, **15**, 433.
Miszalski, B., Acker, A., Moffat, A.F.J., Parker, Q.A., and Udalski, A. 2009, *A&A*, **496**, 813.
Naoz, S., and Fabrycky, D.C. 2014, *ApJ*, **793**, 137.
Nataf, D.M., Gould, A., Fouqué, P., *et al.* 2013, *ApJ*, **769**, 88.
Nefs, S.V., Birkby, J.L., Snellen, I.A.G., *et al.* 2012, *MNRAS*, **425**, 950.
Norton, A.J., Payne, S.G., Evans, T., *et al.* 2011, *A&A*, **528**, A90.
Norton, A.J., Wheatley, P.J., West, R.G., *et al.* 2007, *A&A*, **467**, 785.
Paczyński, B. 1976, in Structure and Evolution of Close Binary Systems (IAU Symposium No. 73), ed. B. Paczyński, P. Eggleton, S. Mitton, and J. Whelan (D. Reidel), 75.
Perets, H.B., and Fabrycky, D.C. 2009, *ApJ*, **697**, 1048.
Pietrukowicz, P., Mróz, P., Soszyński, *et al.* 2013, *Acta Astron.*, **63**, 115.
Pilecki, B. 2010, PhD thesis.
Pilecki, B., Fabrycky, D., and Poleski, R. 2007, *MNRAS*, **378**, 757.
Pilecki, B., and Stępień, K. 2012, *IBVS*, **6012**, 1.
Połubek, G., Pigulski, A., Baran, A., and Udalski, A. 2007, in ASP Conf. Ser. 372, 15th European Workshop on White Dwarfs, ed. N. Ralf and R.B. Matthew (San Francisco, CA: ASP), 487.

Randich, S., Schmitt, J.H.M.M., Prosser, C.F., and Stauffer, J.R. 1996, *A&A*, **305**, 785.
Remillard, R.A., Stroozas, B.A., Tapia, S., and Silber, A. 1991, *ApJ*, **379**, 715.
Riaz, B., Gizis, J.E., and Harvin, J. 2006, *AJ*, **132**, 866.
Rucinski, S.M. 1992, *AJ*, **103**, 960.
Schlegel, D.J., Finkbeiner, D.P., and Davis, M. 1998, *ApJ*, **500**, 525.
Schwarzenberg-Czerny, A. 1996, *ApJ*, **460**, L107.
Smak, J. 1994a, *Acta Astron.*, **44**, 45.
Soszyński, I., Udalski, A., Szymański, M.K., *et al.* 2014, *Acta Astron.*, **64**, 177.
Stępień, K. 2006a, *Acta Astron.*, **56**, 199.
Stępień, K. 2006b, *Acta Astron.*, **56**, 347.
Stępień, K. 2011, *Acta Astron.*, **61**, 139.
Szymański, M., Kubiak, M., and Udalski, A. 2001, *Acta Astron.*, **51**, 259.
Torres, G., Andersen, J., and Giménez, A. 2010, *A&ARv*, **18**, 67.
Tylenda, R., Hajduk, M., Kamiński, T., Udalski, A., Soszyński, I., Szymański, M.K., Kubiak, M., Pietrzyński, G., Poleski, R., Wyrzykowski, Ł., and Ulaczyk, K. 2011, *A&A*, **528**, A114.
Udalski, A., Szymański, M., Kałużny, J., Kubiak, M., Mateo, M., and Krzemiński, W. 1995, *Acta Astron.*, **45**, 1.
Udalski, A. 2003a, *Acta Astron.*, **53**, 291.
Udalski, A. 2003b, *ApJ*, **590**, 284.
Udalski, A., Szymański, M.K., Soszyński, I., and Poleski, R. 2008, *Acta Astron.*, **58**, 69.
Warner, B. 1995, "Cataclysmic Variable Stars" (Cambridge University Press).
Wilson, R.E., and Devinney, E.J. 1971, *ApJ*, **166**, 605.
Wood, J., Horne, K., Berriman, G., Wade, R., O'Donoghue, D., and Warner, B. 1986, *MNRAS*, **219**, 629.
Wood, J.H., Zhang, E.-H., and Robinson, E.L. 1993, *MNRAS*, **261**, 103.
Woźniak, P.R. 2000, *Acta Astron.*, **50**, 421.
Zorotovic, M., and Schreiber, M.R. 2013, *A&A*, **549**, A95.